(34) D. L. Kepert, *Inorg. Chem.*, **11**, 1561 (1972).
(35) S. S. Eaton, I. R. Hutchison, R. H. Hohm, and E. L. Muetterties, *J. Am. Chem. Soc.*, **94**, 6411 (1972).
(36) M. C. Palazzato, D. J. Duffy, B. L. Edgar, L. Zue, Jr., and L. H. Pignolet, *J. Am. Chem. Soc.*, **94**, 6411 (1972).
(37) J. N. van Niekerk and F. R. L. Schoening, *Acta Crystallogr.*, **4**, 35 (1951).
(38) C. A. Bunton, J. H. Carter, D. R. Llewellyn, C. O'Connor, A. L. Odell, and S. Y. Yih, *J. Chem. Soc.*, 4615 (1964).
(39) J. A. Broomhead, I. Lauder, and P. Nimmo, *Chem. Commun.*, 652 (1969).
(40) A. L. Odell, R. W. Olliff, and D. R. Rands, *J. Chem. Soc., Dalton Trans.*, 752 (1972).
(41) A. L. Odell, R. W. Olliff, and F. B. Seaton, *J. Chem. Soc.*, 2280 (1965).
(42) G. K. Schweitzer and J. L. Rose, *J. Phys. Chem.*, **56**, 428 (1952).
(43) S. T. Spees and A. W. Adamson, *Inorg. Chem.*, **1**, 531 (1962).
(44) A. L. Odell and D. Shooter, *J. Chem. Soc., Dalton Trans.*, 135 (1972).
(45) V. S. Sastri and C. K. Langford, *J. Phys. Chem.*, **74**, 3945 (1970).
(46) M. Billardon, *J. Chim. Phys. Phys.-Chim. Biol.*, **62**, 273 (1965).
(47) S. D. Hamann, Paper 3, CSIRO (Austral), Div. App. Chem. Tech., 1972.
(48) W. Kauzmann, A. Bodanszky, and J. Rasper, *J. Am. Chem. Soc.*, **84**, 1777 (1962).
(49) R. M. Noyes, *J. Am. Chem. Soc.*, **86**, 971 (1964).
(50) A. M. Couture and K. J. Laidler, *Can. J. Chem.*, **34**, 1209 (1956).
(51) T. W. Swaddle and P.-C. Kong, *Can. J. Chem.*, **48**, 3223 (1970).
(52) N. Vanderhoek and D. R. Stranks, *J. Chem. Soc., Dalton Trans.*, in press.
(53) T. Kurucesv, A. M. Sargeson, and B. O. West, *J. Phys. Chem.*, **61**, 1567 (1957).

Notes

Contribution from the Department of Chemistry,
Northwestern University, Evanston, Illinois 60201

Structure of Tris(*N,N*-dimethylthiocarbamato)iron(III), Fe(SOCN(CH$_3$)$_2$)$_3$

J. Ahmed and James A. Ibers*

Received November 9, 1976 AIC608136

Extensive studies of tris-chelate complexes of a variety of metals have yielded reasonably firm mechanistic information on the nature of their rearrangement reactions.[1] Such information is based on ground-state geometries, as determined by diffraction methods, and on kinetic parameters. All tris chelates of the type M(AA)$_3$ appear to show at least D_3 idealized symmetry.[2] The twist angle, φ, which is the projection of the bite angle, α, onto a plane perpendicular to the C_3 symmetry axis, may be used for a partial description of geometry. The trigonal prism (symmetry D_{3h}) has the ligand triangles eclipsed and thus has φ of 0°, while the trigonal antiprism (and possible octahedron of symmetry O_h) has the ligand triangles staggered and thus has φ of 60°.

The β-diketonates and the dithiocarbamates are the most studied of these tris chelates. These two types show interesting structural and mechanistic differences. The β-diketonates have φ near 60° and rearrange by bond-rupture pathways; the dithiocarbamates have φ near 38° and rearrange via a trigonal-twist pathway.[1] Yet there is at present no totally satisfying understanding of the influence of solid state geometry on dynamics.[1] Thus additional studies, both mechanistic and structural, especially on new tris-chelate systems, are needed.

Generally the chemical and structural properties of the (mono)thiocarbamate–metal complexes differ markedly from those of the corresponding dithiocarbamates.[3] It is significant, then, that very recently[4] Nakajima et al. described the preparation of tris(thiocarbamato)iron(III) complexes. These complexes are apparently the first, simple tris(thiocarbamate) complexes to be prepared. With the expectation that such complexes will be of interest mechanistically and that interpretation of kinetic data will require knowledge of ground-state structures, the present note establishes the ground-state geometry of one such complex, tris(*N,N*-dimethylthiocarbamato)iron(III).

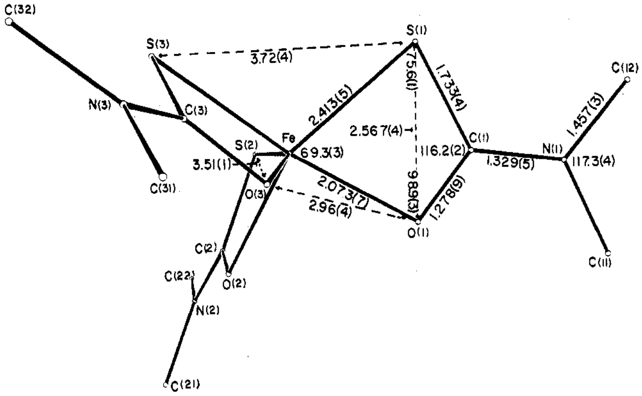

Figure 1. A sketch of the Fe(SOCN(CH$_3$)$_2$)$_3$ molecule showing the labeling scheme and principal, average bond distances and angles.

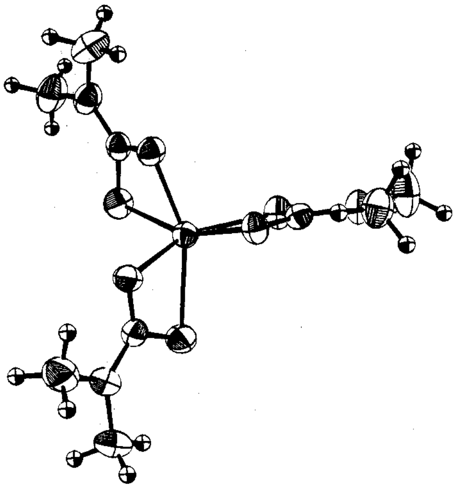

Figure 2. A drawing of the Fe(SOCN(CH$_3$)$_2$)$_3$ molecule displaying vibrational ellipsoids at their 50% level, except for hydrogen atoms which have been drawn artificially small. In the drawing the O(1)–O(2)–O(3) triangle is closer to the viewer than is the S(1)–S(2)–S(3) triangle.

Experimental Section

Suitable crystals of tris(*N,N*-dimethylthiocarbamato)iron(III), Fe(SOCN(CH$_3$)$_2$)$_3$, were kindly supplied by Professor Toshio Tanaka. The crystal structure determination followed experimental and calculational procedures standard in this laboratory.[5] The dark-violet, air-sensitive crystals belong to the triclinic system with a = 9.329 (3), b = 11.571 (4), c = 8.880 (2) Å, α = 102.92 (2), β = 116.13 (2), γ = 95.17 (2)°, V = 811.2 Å^3 (λ(Mo Kα_1) = 0.70930 Å), ρ_c = 1.507 g/cm^3 for two molecules of C$_9$H$_{18}$FeN$_3$O$_3$S$_3$ per cell, ρ_o = 1.49(1) g/cm^3. A total of 3923 unique reflections were collected by diffractometer methods out to 55° in 2θ (Mo Kα); of these 3279 have $F_o^2 > 3\sigma(F_o^2)$ and were used in subsequent calculations. These data were corrected for absorption effects; transmission factors ranged from 0.565 to 0.740 for a crystal of calculated volume 0.139 mm^3 and a linear absorption coefficient of 13.0 cm^{-1}. The structure was solved by Patterson methods and refined by full-matrix, least-squares techniques. Space group C_i^1-$P\bar{1}$ was assumed; this assumption is justified by the eventual location in a difference Fourier map of all hydrogen atoms on the methyl carbon atoms. These hydrogen atoms were placed in idealized positions (C–H = 0.95 Å) and added as fixed contributions in the final cycle of refinement. This cycle of 172

Table I. Positional and Thermal Parameters for the Atoms of $Fe(SOCN)CH_3)_2)_3$

ATOM	X[A]	Y	Z	B11[B]	B22	B33	B12	B13	B23
FE	-0.163155(33)	0.216181(25)	0.034197(35)	104.59(48)	62.64(27)	124.16(54)	13.39(25)	54.98(38)	22.64(27)
S(1)	0.030705(69)	0.130282(46)	-0.045456(76)	140.83(87)	52.19(40)	200.5(11)	19.23(46)	89.53(80)	17.67(51)
S(2)	-0.405562(71)	0.054072(51)	-0.123379(78)	144.79(92)	70.37(48)	190.7(11)	-0.05(51)	74.52(83)	36.93(58)
S(3)	-0.063172(74)	0.193951(57)	0.325537(75)	161.67(97)	95.55(56)	163.8(10)	52.16(59)	79.89(82)	61.54(61)
O(1)	0.02201(17)	0.35242(12)	0.07081(18)	119.8(21)	54.9(11)	163.1(26)	15.7(12)	79.0(20)	18.0(14)
O(2)	-0.32887(17)	0.24646(13)	-0.19448(18)	111.3(22)	65.0(12)	141.0(24)	4.9(13)	47.9(19)	23.5(14)
O(3)	-0.22749(18)	0.34293(14)	0.18681(18)	136.3(24)	83.1(13)	118.8(23)	36.8(15)	63.7(19)	33.9(14)
N(1)	0.24120(21)	0.33580(16)	0.02161(24)	105.5(25)	67.0(15)	185.5(34)	13.2(16)	76.4(25)	23.8(18)
N(2)	-0.57760(22)	0.12962(17)	-0.40506(24)	110.8(27)	81.1(17)	158.8(33)	11.0(17)	43.0(25)	8.4(19)
N(3)	-0.16554(23)	0.37756(18)	0.47144(22)	144.8(30)	95.5(18)	127.8(29)	27.6(19)	70.5(25)	31.4(19)
C(1)	0.10519(23)	0.28579(17)	0.02125(23)	107.7(28)	57.2(15)	112.3(29)	18.6(17)	45.0(24)	20.3(17)
C(2)	-0.44225(24)	0.15034(18)	-0.25351(26)	111.1(29)	61.8(16)	142.2(34)	18.1(17)	68.7(27)	11.3(19)
C(3)	-0.16090(23)	0.31516(19)	0.32912(25)	96.5(27)	76.0(18)	126.9(32)	10.8(18)	46.3(25)	30.2(20)
C(11)	0.29321(29)	0.46783(21)	0.07260(34)	135.2(36)	72.4(19)	230.8(50)	-0.6(21)	79.1(35)	31.1(25)
C(12)	0.33770(34)	0.26307(27)	-0.03618(44)	165.6(46)	107.7(28)	376.7(82)	34.4(29)	174.4(54)	28.9(39)
C(21)	-0.59717(33)	0.21407(27)	-0.50902(34)	168.0(44)	115.2(28)	182.4(47)	37.4(29)	28.6(37)	44.5(30)
C(22)	-0.71287(29)	0.02426(25)	-0.47406(37)	123.9(35)	94.7(24)	238.2(54)	-10.4(23)	40.9(35)	-7.0(29)
C(31)	-0.25066(34)	0.47789(25)	0.46535(33)	205.2(48)	105.1(25)	175.6(44)	48.2(29)	102.1(39)	25.0(27)
C(32)	-0.08793(35)	0.35094(28)	0.63829(30)	210.4(49)	140.1(31)	127.9(38)	41.1(32)	80.9(36)	47.6(28)

[A] ESTIMATED STANDARD DEVIATIONS IN THE LEAST SIGNIFICANT FIGURE(S) ARE GIVEN IN PARENTHESES IN THIS AND ALL SUBSEQUENT TABLES. [B] THE FORM OF THE ANISOTROPIC THERMAL ELLIPSOID IS: EXP[-(B11H^2+B22K^2+B33L^2+2B12HK+2B13HL+2B23KL)]. THE QUANTITIES GIVEN IN THE TABLE ARE THE THERMAL COEFFICIENTS X 10^4.

Table V. Details of the Inner FeS_3O_3 Core in $Fe(SOCN(CH_3)_2)_3$

Distances, Å		
Fe-S(1)	2.412 (1)	2.413 (5)[a]
Fe-S(2)	2.409 (1)	
Fe-S(3)	2.418 (1)	
Fe-O(1)	2.076 (2)	2.073 (7)
Fe-O(2)	2.066 (2)	
Fe-O(3)	2.078 (2)	
S(1)· · ·O(1)	2.570 (2)	2.567 (4)
S(2)· · ·O(2)	2.568 (2)	
S(3)· · ·O(3)	2.563 (2)	
S(1)· · ·O(2)	3.510 (2)	3.510 (8)
S(2)· · ·O(3)	3.517 (2)	
S(3)· · ·O(1)	3.502 (2)	
S(1)· · ·S(2)	3.759 (2)	3.72 (4)
S(1)· · ·S(3)	3.701 (2)	
S(2)· · ·S(3)	3.689 (2)	
O(1)· · ·O(2)	2.971 (2)	2.96 (4)
O(1)· · ·O(3)	2.913 (2)	
O(2)· · ·O(3)	2.986 (2)	
$S_{ct}\cdots O_{ct}$[b]	2.281	

Bond angles, deg		
S(1)-Fe-O(1)	69.38 (5)	69.3 (3) = α
S(2)-Fe-O(2)	69.57 (5)	
S(3)-Fe-O(3)	69.02 (5)	
Interplanar angle, deg		
S(1)-S(2)-S(3) O(1)-O(2)-O(3)	0.86	
Vector-plane angles, deg		
S_{ct}-O_{ct} S(1)-O(1)-C(1)	64.5	64.7 = 90 − Ψ[c]
S_{ct}-O_{ct} S(2)-O(2)-C(2)	63.6	
S_{ct}-O_{ct} S(3)-O(3)-C(3)	66.0	
Intervector angles, deg		
S_{ct}-S(1) O_{ct}-O(1)	33.3	33.2 = φ
S_{ct}-S(2) O_{ct}-O(2)	34.0	
S_{ct}-S(3) O_{ct}-O(3)	32.3	

[a] The standard deviation of an average quantity is for a single observation and is the larger of that estimated from the inverse matrix or from the agreement among the quantities averaged on the assumption that they are from the same population. [b] S_{ct} is the center of the S triangle (average of the S coordinates); O_{ct} is defined similarly with respect to the O triangle. [c] The pitch angle ψ is defined by L.H. Pignolet, *Inorg. Chem.*, 13, 2051 (1974), as the angle between the plane of the chelate ring and the C_3 axis. This is the complement of the angle defined here as that between the normal to the plane and the C_3 axis.

variables converged to conventional and weighted agreement indices on F of 0.029 and 0.044, respectively, and to an error in an observation of unit weight of 1.69 e. The largest peak on a final difference Fourier map (0.3 e/Å^3) is about 8% of the height of a typical C atom peak on early maps. No unusual trends in $\sum w(|F_o| - |F_c|)^2$ were found as a function of setting angles, $|F_o|$, or Miller indices.

Final positional and thermal parameters for the nonhydrogen atoms are given in Table I. Table II[6] contains the positions of the hydrogen atoms. Root-mean-square amplitudes of vibration are given in Table III.[6] Values of $10|F_o|$ vs. $10|F_c|$ are given in Table IV.[6]

Discussion

The structure of $Fe(SOCN(CH_3)_2)_3$ consists of well-separated molecules. The Fe atom is coordinated to three, virtually planar thiocarbamate groups. Although the molecule cannot possess a D_3 symmetry axis, owing to the dissimilar liganding atoms, the isomer studied here does possess a reasonable C_3 axis, with the plane of the three S atoms being virtually parallel to that of the three O atoms (dihedral angle, 0.86°; see Table V). Figure 1 displays the labeling scheme as well as some important average distances and angles. Figure 2 shows a complete molecule.

Bond distances and angles within the thiocarbamate ligands are unremarkable and resemble closely those found in other thiocarbamate and dithiocarbamate complexes.[3,7]

Of principal interest is the geometry of the inner FeS_3O_3 core, and details of this geometry are given in Table V. The present complex exhibits an average Fe–S distance (2.413 (5) Å) that is significantly longer than that observed at room temperature in tris(*N*,*N*-diethyldithiocarbamato)iron(III)[7] (2.358 (6) Å). The bite angles in the two complexes are, as expected, different. Otherwise the complexes are very similar. Thus the twist angle (φ) and pitch angle (ψ)[8] for the thio- and dithiocarbamate complexes are respectively 33.2 and 25.3° vs. 37.6 and 26.8°. In fact, the average values of φ and ψ in a series of nine tris(dithiocarbamate) metal complexes are 38.2 and 27.8°, respectively.[1] Thus both the present tris(thiocarbamate) complex and a variety of tris(dithiocarbamate) complexes display similar geometries, intermediate between the trigonal prism and the pseudooctahedron. This intermediate geometry clearly cannot be ascribed to the presence of the FeS_6 core. Despite this close geometrical resemblance, tris(thiocarbamato)iron(III) and tris(dithiocarbamato)iron(III) differ in their magnetic properties, with the thiocarbamate complex showing a simple high-spin state[4] while the dithiocarbamate complex lies at the crossover between high-spin and low-spin states.[9] Whether or not the rearrangement mechanisms are also different is yet to be determined.

Acknowledgment. This research was supported by UNESCO. J.A. acknowledges with thanks receipt of a UNESCO Fellowship. We are indebted to Professor Toshio Tanaka for supplying the crystals.

Registry No. $Fe(SOCN(CH_3)_2)_3$, 61375-77-7.

Supplementary Material Available: Table II, the positions of the H atoms; Table III, the root-mean-square amplitudes of vibration; and Table IV, a listing of observed and calculated structure amplitudes (25 pages). Ordering information is given on any current masthead page.

References and Notes

(1) L. H. Pignolet, *Top. Curr. Chem.*, **56**, 91 (1975).
(2) E. L. Muetterties and L. J. Guggenberger, *J. Am. Chem. Soc.*, **96**, 1748 (1974).
(3) C. G. Pierpont, R. C. Dickinson, and B. J. McCormick, *Inorg. Chem.*, **13**, 1674 (1974).
(4) H. Nakajima, T. Tanaka, H. Kobayashi, and I. Tsujikawa, *Inorg. Nucl. Chem. Lett.*, **12**, 689 (1976).
(5) See, for example, P. R. Hoffman, T. Yoshida, T. Okano, S. Otsuka, and J. A. Ibers, *Inorg. Chem.*, **15**, 2462 (1976).
(6) Supplementary material.
(7) J. G. Leipoldt and P. Coppens, *Inorg. Chem.*, **12**, 2269 (1973).
(8) L. H. Pignolet, *Inorg. Chem.*, **13**, 2051 (1974).
(9) A. H. White, E. Kokot, R. Roper, H. Waterman, and R. L. Martin, *Aust. J. Chem.*, **17**, 294 (1964); A. H. Ewald, R. L. Martin, E. Sinn, and A. H. White, *Inorg. Chem.*, **8**, 1837 (1969).

Contribution from Rocketdyne, A Division of
Rockwell International, Canoga Park, California 91304

Synthesis and Characterization of NF_4BiF_6 and Some Properties of NF_4SbF_6

Karl O. Christe,* Richard D. Wilson, and Carl J. Schack

Received March 9, 1976 AIC60186K

Perfluoroammonium salts are known[1] of the following anions: PF_6^-, AsF_6^-, SbF_6^-, $SbF_6{\cdot}nSbF_5^-$, BF_4^-, GeF_5^-, and GeF_6^{2-}. Very recently, the synthesis and chemistry of NF_4^+ salts have received considerable attention owing to their potential for solid propellant NF_3–F_2 gas generators for chemical DF lasers. The concept of such a gas generator was conceived[2] and to a large extent developed at Rocketdyne. Originally, the fluorine gas generators were aimed at the direct generation of F atoms by burning a highly overoxidized grain, consisting mainly of an NF_4^+ salt, with a small amount of fuel, such as Teflon powder, according to

$$NF_4MF_6 + (CF_2)_n \rightarrow CF_4 + NF_3 + MF_5 + Q$$

$$NF_4MF_6 \xrightarrow{+Q} NF_3 + F_2 + MF_5$$

$$2NF_3 + F_2 \xrightarrow{+Q} N_2 + 8F\cdot$$

The heat of reaction (Q) generated in such a system is sufficient to pyrolyze the remaining NF_4MF_6 and to dissociate most of the NF_3 and F_2 to F atoms. For an NF_3–F_2 gas generator, the underlying principle is quite similar, except for keeping the burning temperature lower since dissociation of NF_3 and F_2 to F atoms is not required.

In view of the above developments, we were interested in the synthesis of new NF_4^+ salts and in the characterization of new and known NF_4^+ salts. In this paper, we report on the synthesis of the new salt NF_4BiF_6 and on some properties of the known NF_4SbF_6. Since these two salts can be readily prepared in high yields, they are important starting materials for the syntheses of other NF_4^+ salts used in NF_3–F_2 gas generator compositions.

Experimental Section

Materials and Apparatus. The equipment and handling procedures used in this work were identical with those[1] recently described. The NF_4BF_4 starting material was prepared by low-temperature UV photolysis[1] and did not contain any detectable impurities. The α-BiF_5 was purchased from Ozark Mahoning Co. and did not contain any impurities detectable by Raman spectroscopy. The $NF_4Sb_2F_{11}$was prepared as described.[3]

Synthesis of NF_4BiF_6 by Displacement Reaction without Solvent. Pure NF_4BF_4 (10.1 mmol) and α-BiF_5 (10.1 mmol) were powdered, mixed, and placed in a prepassivated (with ClF_3) 95-mL Monel cylinder. The cylinder was heated to 180 °C for 1.5 h. Products, volatile at 20 °C, were removed by pumping and separated by fractional condensation. They consisted of 7.8 mmol of BF_3 in addition to a small amount of material noncondensable at −196 °C. The amount of BF_3 evolution was confirmed by the weight loss of the solid-containing cylinder. The conversion of NF_4BF_4 to NF_4BiF_6 was further confirmed by Raman spectroscopy of the solid. The solid was removed from the cylinder, finely powdered, returned to the cylinder, and heated to 175 °C for an additional 18 h. This resulted in the evolution of an additional 2.3 mmol of BF_3, in excellent agreement with the observed weight loss. The complete conversion of NF_4BF_4 to NF_4BiF_6 was confirmed by infrared and Raman spectroscopy and elemental analysis. Anal. Calcd for NF_4BiF_6: NF_3, 17.15; BiF_3, 64.49. Found: NF_3, 16.9; BiF_3, 60.0 An explanation for the low BiF_3 value is given below.

Synthesis of NF_4BiF_6 by Displacement Reaction in HF. Dry HF (5 mL of liquid) was added at −78 °C to a Teflon–FEP ampule containing NF_4BF_4 and BiF_5 (9.9 mmol of each). The mixture was agitated at 20 °C for several hours and gas evolution was observed. The volatile products were pumped off at 20 °C and the HF treatment was repeated. After removal of the volatile products from the second HF treatment, 4.075 g of a white, stable solid (weight calculated for 9.9 mmol of NF_4BiF_6 4.089 g) was left behind which was shown by infrared and Raman spectroscopy to be identical with the analyzed product obtained from the above described thermal displacement reaction.

Direct Synthesis of $NF_4BiF_6{\cdot}nBiF_5$. In a typical experiment, a mixture of NF_3 (238 mmol), F_2 (238 mmol), and BiF_5 (10.06 mmol) in a prepassivated 95-mL Monel cylinder was heated for 30 h to 175 °C under an autogenous pressure of 167 atm. Unreacted NF_3 and F_2 (~463 mmol total) were pumped off at 20 °C leaving behind 3.75 g of a white, stable solid (weight calculated for 6.29 mmol of $NF_4BiF_6{\cdot}0.6BiF_5$ 3.745 g). Anal. Calcd for $NF_4BiF_6{\cdot}0.6BiF_5$: NF_3, 11.92; BiF_3, 71.60. Found: NF_3, 11.9; BiF_3, 69.00.

Pyrolysis of $NF_4BiF_6{\cdot}nBiF_5$. A sample (3.29 mmol) of $NF_4BiF_6{\cdot}1.46BiF_5$, prepared as described above expept for using a significantly shorter reaction time, was subjected to vacuum pyrolysis at 280 °C for 1.5 h. The white crystalline residue (1.13 g) was identified by vibrational spectroscopy and its x-ray diffraction powder pattern to be mainly NF_4BiF_6 (weight calculated for 3.29 mmol of NF_4BiF_6 1.36 g) corresponding to a yield of 83%.

Synthesis of NF_4SbF_6. The thermal reaction[4] of NF_3–F_2–SbF_5 at 115 °C, followed by vacuum pyrolysis at 200 °C, produces[3] a product of the approximate composition $NF_4Sb_2F_{11}$. This product can be converted to NF_4SbF_6 by vacuum pyrolysis at higher temperature; however, this SbF_5 removal is accompanied by a competing reaction, i.e., the thermal decomposition of some of the desired NF_4SbF_6. Pyrolysis at 250–260 °C for 1–1.5 h under dynamic vacuum resulted in complete conversion to NF_4SbF_6. Measurement of the NF_3 evolved during this pyrolysis showed that less than 3% of the NF_4SbF_6 had undergone decomposition. When the pyrolysis was carried out at 275–300 °C, even for relatively short periods of time, significantly